

A Statistical Model for Estimation of Soil Moisture in Paddy Field Using Microwave Satellite Data

Packirisamy Pari^{1, *}, Packirisamy Thirumaraiselvan¹,
Murugaiyan Ramalingam², and Shanmugam Jayalakshmi³

Abstract—Estimation of soil moisture using Synthetic Aperture Radar (SAR) backscatter values, over agricultural area, is still difficult. SAR backscatter is sensitive to the surface properties like roughness, crop cover, and soil type, along with its strong sensitivity to soil moisture. Hence, to develop a methodology for agricultural area soil moisture estimation using SAR, it is necessary to incorporate the effects of crop cover and soil texture in the soil moisture retrieval model. A field experiment was conducted by the authors and used along with Sentinel 1A SAR data to estimate the soil moisture in the paddy agricultural fields. Generally, the water used for irrigation in the study region was obtained from ground water. As in the hot climate conditions ground water level would be reduced, and the water for irrigation must be supplied optimally. Hence, available soil moisture in the field was estimated from SAR data on the day of satellite passing the crop fields and utilized for deciding the amount of water to be supplied. The soil moisture values of soil samples that are collected from the agricultural field are calculated with the laboratory experiments. A soil moisture retrieval model is derived and proposed in this paper after a comparative analysis of experimental soil moisture values and satellite values. The feasibility of above model for paddy agricultural fields is validated using the field measurements.

1. INTRODUCTION

The soil moisture is one of the most important parameters that could be retrieved with remote sensing technology and used in hydrological modelling, ecological monitoring, and change analysis [1]. Remote sensing provides us an opportunity to assess and monitor the water usage based on the retrieved soil moisture at regional and large level scales [2, 3]. Soil moisture estimation by optical, thermal, and microwave remote sensing methods have been proposed for the past 35 years. Many approaches have been established by the relationships between soil reflectivity and soil moisture and also surface thermal properties with soil moisture [4, 5]. Remote sensing systems using microwave sensors could be classified as active and passive [6]. All existing objects or surface in the earth emit microwave energy, but its magnitude is generally very small. This energy is emitted from the object or surface according to its properties such as atomic composition, crystalline structure, temperature, and moisture. A passive microwave sensor system is used to detect this naturally emitted microwave energy within its field of view. Passive system has highly sensitive radiometers which measure the microwave radio emission of the materials at a particular wavelength.

Active radar remote sensing, which has the advantages over passive optical remote sensing, has its own source of illumination and penetrates vegetation layers up to a few centimetre depth of soil, so it can collect the information underlying vegetation soil moisture [7]. Thus it is possible to collect information under any weather condition and also penetration through clouds [8–10]. The frequency

Received 14 May 2020, Accepted 1 July 2020, Scheduled 21 July 2020

* Corresponding author: Packirisamy Pari (pari15683@gmail.com).

¹ Adhiparasakthi Engineering College, Tamilnadu, India. ² Jerusalem College of Engineering, Tamilnadu, India. ³ Institute of Remote Sensing, Anna University Chennai, Tamilnadu, India.

band from 0.3 GHz to 300 GHz is used by the active remote sensing systems corresponding to wavelengths between 1 mm and 1 m [11]. For instance, the X-band with 2.4–3.75 cm wavelength is reflected by the surface objects. The C-band with 3.75–7.5 cm wavelength only reaches the parts that are immediately near the surface. The L-band with a wavelength range of 15–30 cm could penetrate through the plants and reach the objects underneath ground. Under dry soil condition, the L-band penetration up to several meters provides us the observation of moisture content. However in many studies, the retrieval of moisture content was investigated not only with longer wave lengths but also with C-band radars (shorter wavelength) [12–14]. The main issue of this microwave system is contrasting problem that occurs while the illuminating source signal is scattered by the soil moisture and the leaf water content [15]. Hence, most of the existing models include field measurements in order to increase the accuracy. In a bare area, soil moisture estimation has been done with geometrical optics model, physical optics model, small perturbation model, etc. [16]. For vegetation areas, Michigan microwave canopy scattering [17], water-cloud model [18], and crop model [19] have been used to estimate the soil moisture. Since soil parameters monitoring large areas using SAR data are very helpful for water management, flood forecasting and drought monitoring [20–23], researchers developed different empirical models [24–26] and semi-empirical models [27, 28] by the relationship between backscattering coefficients and soil moisture.

Soil moisture measurement is necessary to enhance the effectiveness of the ecological protection such as soil-water conservation, land reclamation, and vegetation restoration [29–32]. Soil moisture estimation in the cropping field mainly depends on wavelength, polarisation, target, and incident angle [33, 34]. The estimation of soil moisture using microwave data in the cropping region is a challenging process because the crop leaves scattered the rays more than the soil in the dense vegetation region [35]. Generally, soil backscattering values in a homogeneous cropping pattern region are estimated using microwave satellite image by applying the Water Cloud Model (WCM) algorithm [36]. To prevent water stress of crops and improve the productivity, monitoring the water availability in the root zone at varying stages of crop growth periods is essential. At agricultural fields, soil moisture data can be measured and used for precision irrigation scheduling [37]. But the conventional method of soil moisture measurement in large scale is expensive, tedious, and time consuming. Hence, remote sensing is used as an alternative tool to estimate the soil properties [38].

A statistical model to derive the soil moisture in paddy agricultural fields is proposed in this paper. The detailed procedure to be followed in the development of the proposed model is shown in Figure 3. This model could be used to prevent the excess use of water supply and reduce the water stress in water scarcity region. Sentinel 1A and Landsat 8 Operational Land Imager (OLI) satellite data are used in this model to find the water availability in the root zone level at different growth periods. The characteristics of the above two satellites are given in Table 1. In order to validate the model, experimental soil moisture at the study region is determined with collected soil samples of the respective region and compared with the derived soil moisture.

Table 1. Characteristics of satellite data.

Satellite details	Landsat 8 OLI	Sentinel 1A
Launch date	11 February 2013	3 April 2014
Resolution	band 4 (30 m), band 5 (30 m)	Pan: 10 m
Altitude	703.0 kilometers	693 kilometers
Inclination	98.2 degree	98.18 degree
Orbit	Sun-synchronous	Sun-synchronous
Polarisation	-	VH/VV

2. STUDY AREA AND DATA COLLECTION

The sample soil pockets were collected from December 2016 to February 2017 at three different paddy fields in the Maduranthagam village, Kanchipuram district, Tamilnadu, India (shown in Figure 1). Two

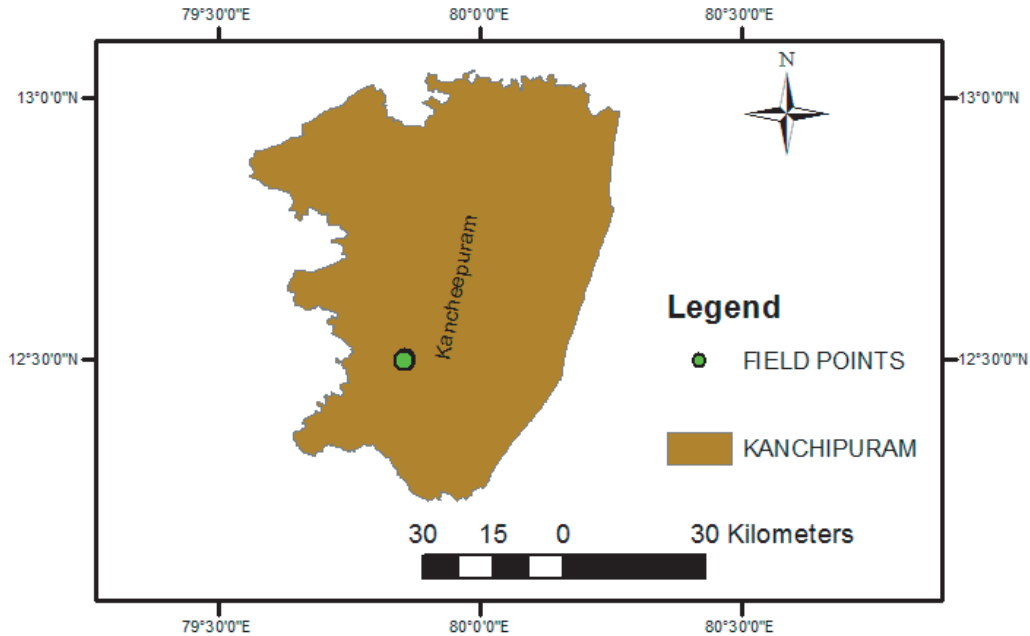


Figure 1. Location of field points.

fields were used for experimental purpose, and one field was used for validating the proposed model. Sentinel 1A dual polarization (VV + VH) mode microwave satellite data were used in this study. The revisit period of Sentinel 1A satellite is 12 days. In the usual manner, the farmer prepared the land for cultivation of paddy. Growth duration of paddy is 45 days. The soil samples were collected from the field, at the time of satellite passing the study region, using metallic cylinder with known volume (100 cm³). The soil samples were collected at the air tight cover with location details. The location was taken from the Trimble Global Positioning System (GPS) with 1 m accuracy. Once in every 12 days the samples were collected at different growth stages of paddy.

3. FIELD MEASURED SOIL MOISTURE

The collected soil samples were dried using oven at 105°C temperature for 24 hours, and the dried samples are shown in Figure 2. From the weights of the wet and dried soil samples, gravimetric soil moisture was estimated and converted into volumetric soil moisture using bulk density.

$$\text{Gravimetric soil moisture } S_g = \frac{W_s - W_d}{W_d}$$



Figure 2. Oven dried soil samples.

$$\text{Bulk density, } \rho_b = \frac{W_s}{V}$$

$$\text{Volumetric soil moisture } S_v = S_g \times \rho_b$$

where,

- W_s = Weight of wet soil sample,
- W_d = Weight of dried sample,
- V = Volume of sample.

4. SOIL MOISTURE FROM SATELLITE IMAGE

Sentinel 1A is a satellite launched by European Space Agency as a part of earth observation mission. It focuses on earth observation such as atmospheric, oceanic, and land monitoring. The image data are available as open source from its official website called as Copernicus Space Component Data Access Portal [39]. In the proposed model, the downloaded Sentinel 1A image data are preprocessed using

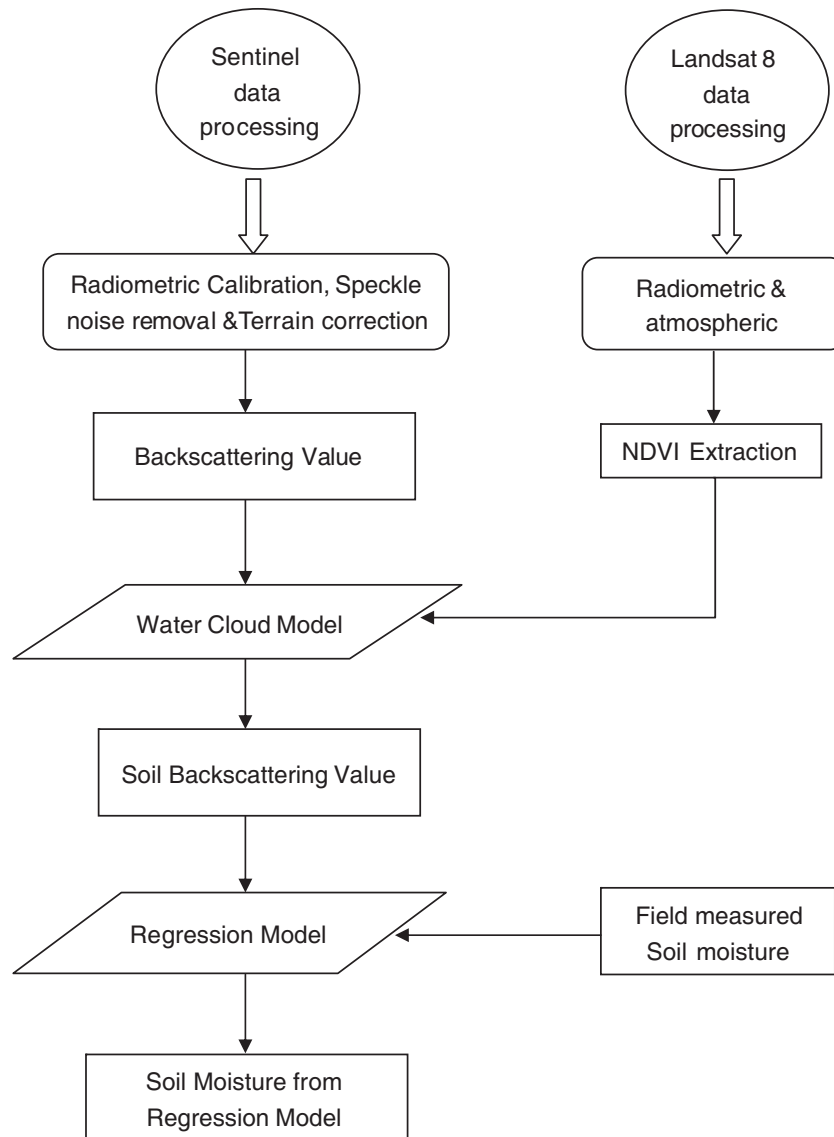


Figure 3. Retrieval of soil moisture from satellite image.

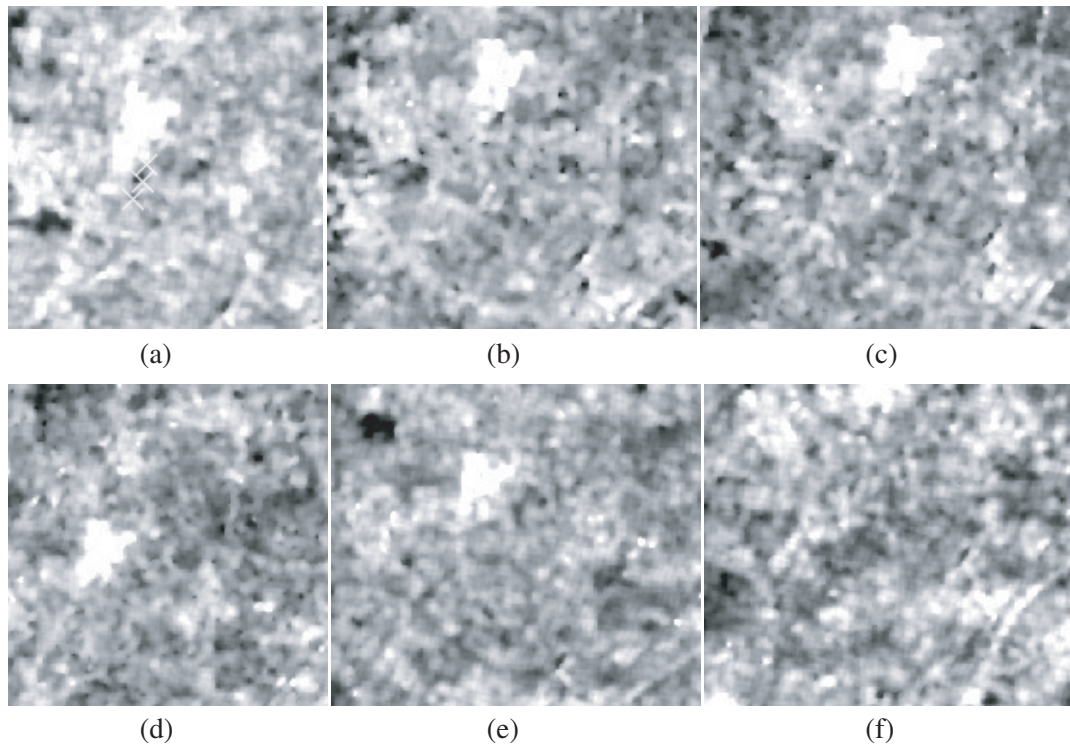


Figure 4. Sentinel 1A satellite data of the study field on different dates. (a) 12-12-2016. (b) 24-12-2016. (c) 05-01-2107. (d) 17-01-2017. (e) 29-01-2017. (f) 10-02-2017.

Lee refined filter to reduce the speckle noise. Then terrain correction is done with Shuttle Radar Topographic Mission (SRTM) 3 second Digital Elevation Model (DEM) data, in order to correct the topographic deformations. The combined back scattering values, which represent the proportion of microwave backscattered from the study area, are extracted from the resultant image. The above process is continued for the entire growth period of paddy on the days of field samples collected, and the preprocessed images are shown in Figure 4. All the above Sentinel 1A image data processed are done using SNAP Toolbox, which is provided by the European Space Agency as an open source.

The geo referenced Landsat 8 OLI satellite data were downloaded [40] and images are rectified into Universal Transverse Mercator (UTM) coordinate system, using World Geodetic System 1984 (WGS 84). The Landsat 8 satellite sensor captures the reflected solar energy from the earth's surface and saves it into 16 bit digital number (DN). Then radiometric correction, conversion of DN value into Top of Atmospheric radiance value (ToAR), is done in the Landsat bands using the following equation in ENVI image analysis software.

$$L_{\lambda} = m * p + a$$

where,

L_{λ} = Spectral radiance (W/(m²*sr*μm)),

m = Radiance multiplicative scaling factor,

a = Radiance additive scaling factor for the band,

p = Pixel value in DN.

The radiance value obtained using the above equation for a particular surface includes the radiation reflected from the surface, neighboring pixels, clouds, and aerosols above the area of the surface. Hence, to nullify these atmospheric effects, radiance image is corrected into reflectance image, which is called as atmospheric correction, using ENVI.

The backscattering values that are extracted from Sentinel 1A image are of vegetation and underlying wet or dry soil. Soil moisture could be determined from the crop underlying soil backscattering values, which are separated from the combined backscattering values. The Water Cloud

Model (WCM) is used to accomplish this task [41] and gives the relation among vegetation, soil, and combined back scattering values.

$$\begin{aligned}\sigma^o &= \sigma_{veg}^o + \tau^2 \sigma_{soil}^o \\ \sigma_{veg}^o &= A m_v \cos \theta (1 - \tau^2) \\ \tau^2 &= e^{(-2B m_v \sec \theta)}\end{aligned}$$

where,

- σ^o = combined backscattering value,
- σ_{veg}^o = vegetation backscattering value,
- σ_{soil}^o = soil backscattering value,
- m_v = vegetation water content,
- θ = Local incidence angle that is extracted from the corrected SAR data,
- τ^2 = two way vegetation transmissivity.

Normalized Difference Vegetation Index (NDVI) values are the indicator of vegetation density. Hence, NDVI is used in the place of A and B parameters, which represent the contribution of vegetation in backscatter values [42]. Generally, NDVI is obtained from the Landsat 8 optical satellite image radiance values of near infrared and red band as given below.

$$NDVI = \frac{Near\ Infraredband - Redband}{Near\ Infraredband + Redband}$$

The vegetation moisture content (m_v) is estimated from laboratory based oven dry method and used in the WCM.

These soil backscattering values are related with field measured soil moisture, and a regression analysis has been done. From the regression analysis, a statistical model, which provides the soil moisture values for the given soil backscattering values, is proposed in this paper. This model is applicable to the paddy fields with sandy clay loam soil. The validity of the proposed model is verified by the comparative analysis of the field measured soil moisture and estimated soil moisture values of another study area of similar soil type. A good agreement observed in the comparative analysis substantiates the consistency of this model.

5. RESULTS AND DISCUSSION

The soil moisture values of different fields were estimated using laboratory oven dry method at different growing stages of paddy crops and shown in Tables 2 to 4. From the initial growing stage to middle growing stage of crops, the moisture content lies between $0.33\text{ cm}^3/\text{cm}^3$ and $0.42\text{ cm}^3/\text{cm}^3$. This is because of higher water supply due to higher leaf transpiration loss, which is higher at the early growing stage of paddy. After the fruit full stage, less water is required due to less transpiration by low greenness effect of crop leaves. Hence, the moisture content value gradually decreases, from fruit full stage to harvesting stage and is found as between $0.31\text{ cm}^3/\text{cm}^3$ and $0.16\text{ cm}^3/\text{cm}^3$. Very low moisture content is noticed at the harvesting stage.

Table 2. Volumetric soil moisture of field 1.

Latitude	Longitude	Date of Sample Collection	Volumetric Soil Moisture in cm^3/cm^3
12° 29'48" N	79° 51'23" E	12-12-2016	0.34
		24-12-2016	0.37
		05-01-2107	0.25
		17-01-2017	0.22
		29-01-2017	0.24
		10-02-2017	0.19

Table 3. Volumetric soil moisture of field 2.

Latitude	Longitude	Date of sample Collection	Volumetric Soil Moisture in cm^3/cm^3
12° 29'52"N	79° 51'25"E	12-12-2016	0.39
		24-12-2016	0.33
		05-01-2107	0.33
		17-01-2017	0.31
		29-01-2017	0.30
		10-02-2017	0.21

Table 4. Volumetric soil moisture of field 3.

Latitude	Longitude	Date of Sample Collection	Volumetric Soil Moisture in cm^3/cm^3
12° 29'56"N	79° 51'26"E	12-12-2016	0.42
		24-12-2016	0.35
		05-01-2107	0.36
		17-01-2017	0.29
		29-01-2017	0.22
		10-02-2017	0.16

The combined backscattering coefficient values were extracted from the Sentinel 1A satellite data and shown in Table 5 on different dates for three different fields. In the first field, values vary from -19.325 to -14.627 , second field from -18.206 to -13.249 , and third field from -17.260 to -16.381 . Higher and lower magnitudes of backscattering coefficient values indicate higher and lower water contents in the soil. But these backscattering values in crop fields are not only of soil reflected one. These values represent the combined effect of crop and soil reflected backscattering. The exact value of soil backscattering that is crop underlying soil backscatter value is the required one in order to take decisions in various irrigation and agricultural practices. The soil backscatter value was estimated from the preprocessed Sentinel 1A satellite data (Figure 4) as explained in section 4 and given in Table 6.

Table 5. Combined Backscattering values of sample locations.

Date	S_1	S_2	S_3
12-12-2016	-19.325	-18.206	-17.260
24-12-2016	-17.627	-18.587	-17.246
05-01-2107	-16.986	-17.071	-17.280
17-01-2017	-17.815	-16.348	-16.281
29-01-2017	-15.101	-14.890	-15.732
10-02-2017	-14.627	-13.249	-16.381

The regression analysis was made between combined as well as soil backscattering values and the soil moisture content (shown in Figures 5 and 6) of study fields S_1 and S_2 . The correlation between combined backscattering coefficient value (σ^o) and soil moisture is found as moderate, and the correlation coefficient value (R^2) is only 0.44 (shown in Figure 5). Conversely, a strong correlation is found between the soil backscattering (σ_{soil}^o) and field measured soil moisture values, and the correlation coefficient value (R^2) is 0.83 (shown in Figure 6). The statistical relation derived from the regression analysis to

Table 6. Soil backscattering values of sample locations.

Date	S_1	S_2	S_3
12-12-2016	-16.064	-17.319	-16.260
24-12-2016	-15.732	-15.172	-15.268
05-01-2107	-14.476	-15.461	-14.566
17-01-2017	-14.151	-14.621	-13.944
29-01-2017	-13.027	-13.736	-13.111
10-02-2017	-11.743	-12.147	-13.204

determine the soil moisture values from the soil backscattering values is given below.

$$\text{Soil Moisture} = -0.036 * \sigma_{soil}^o - 0.244$$

There is no generalized soil moisture estimation model available in the literature for paddy crop regions. But a few models are available in literature for general cropping filed irrespective of the crop

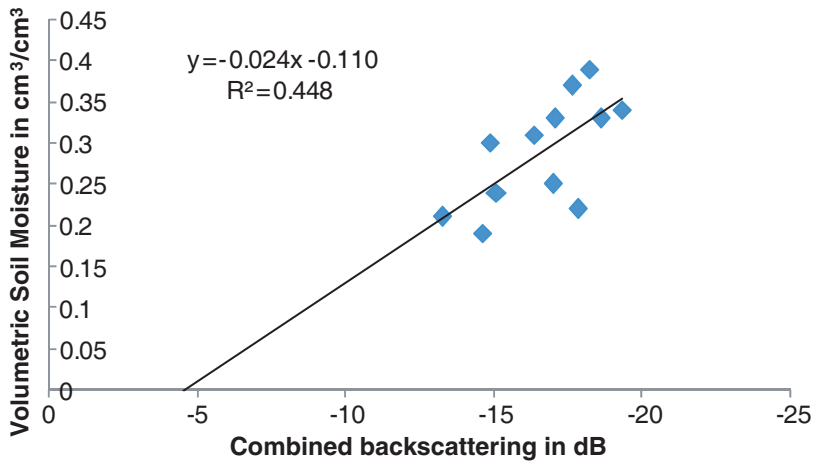


Figure 5. Relation between combined backscattering values and soil moisture.

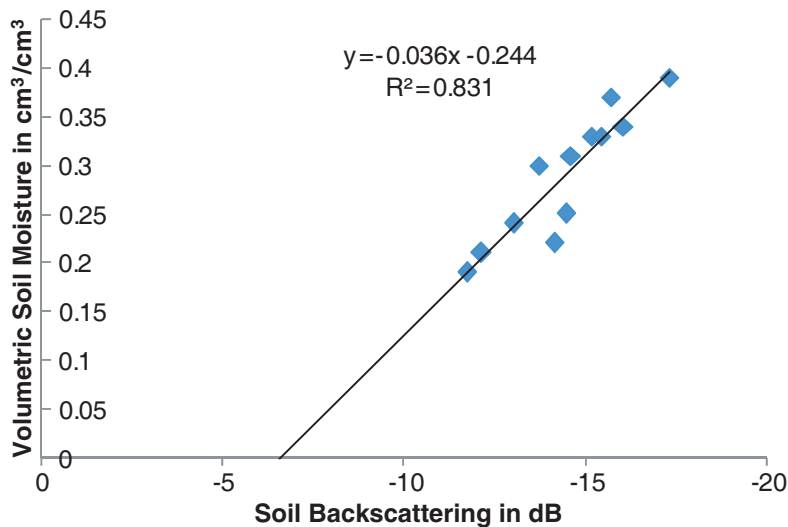


Figure 6. Relation between soil backscattering values and soil moisture.

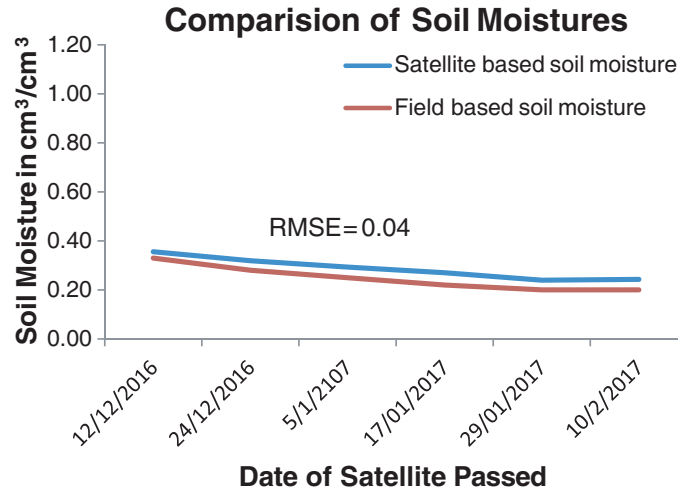


Figure 7. Comparison of field measured and satellite image based soil moisture.

type. In [43], bare soil data with no vegetation have been used to propose a generalized model. The accuracy assessment has been conducted using 7 test sites, and the statistical metrics, namely R^2 and RMSE, were determined as 0.84 and 0.0246, respectively. However, the outcomes are incomparable as both of the models are developed based on empirical soil moisture values that depend on the geological properties of the study area and the time in which the SAR data were collected. Hence, in order to validate the proposed model, field based soil moistures of the samples collected from the study area S_3 were used (shown in Figure 7). The variation of the estimated soil moisture values from the actual field based soil moistures is around $0.02 \text{ cm}^3/\text{cm}^3$ to $0.05 \text{ cm}^3/\text{cm}^3$ only. The Root Mean Square Error (RMSE) between the soil moisture values of these two methods is observed as 0.04. This ensures the applicability of the proposed model for soil moisture estimation in paddy fields with sandy clay loam soil.

6. CONCLUSION

In this paper, an empirical soil moisture model has been proposed in order to estimate the soil moisture from the soil backscattering values that could be extracted from SAR data. This model could be used to prevent the excessive use of water supply to the paddy agricultural fields and to reduce the water stress in water scarcity region according to the soil moisture value of the respective region. Sentinel 1A and Landsat 8 Operational Land Imager (OLI) satellite data are used in this model to find the soil moisture in the root zone level at different growth periods. From the regression analysis, it is found that soil moisture has strong correlation with soil backscatter values compared to combined backscatter values. Hence, the proposed model has been derived by the regression analysis with field measured soil moisture and soil backscatter values. Validation of the proposed model has been done by the comparative analysis between the field measured moisture content and the model based moisture content. The error between these two soil moistures lies within $0.02\text{--}0.05 \text{ cm}^3/\text{cm}^3$. The RMSE is observed as 0.04, which proves the applicability and reliability of the proposed model for paddy agricultural fields. This study may be further extended to the areas with mixed land cover or mixed crop region and to different climate zone regions. It will be more meaningful in terms of dynamic monitoring and evolution prediction of ecosystem.

REFERENCES

1. Zhang, D., Z. L. Li, R. Tang, B. H. Tang, H. Wu, J. Lu, and K. Shao, "Validation of a practical normalized soil moisture model with in situ measurements in humid and semi-arid regions," *International Journal Remote Sensing*, Vol. 36, 5015–5030, 2015.

2. Abuzar, M., A. McAllister, D. Whitfield, and K. Sheffield, "Remote sensing analysis of crop water use in the macalister irrigation district," *Geospatial Science Research*, 1–7, 2012.
3. Li, Z.-X., "Modelling the passive microwave remote sensing of wet snow," *Progress In Electromagnetics Research*, Vol. 62, 143–164, 2006.
4. Awe, G. O., J. M. Reichert, L. C. Timm, and O. O. Wendroth, "Temporal processes of soil water status in a sugarcane field under residue management," *Plant Soil*, Vol. 387, 395–411, 2015.
5. Chen, X. Z., S. S. Chen, R. F. Zhong, Y. X. Su, J. S. Liao, D. Li, L. Han, Y. Lia, and X. A. Li, "Semi-empirical inversion model for assessing surface soil moisture using AMSR-E brightness temperatures," *Journal of Hydrology*, Vol. 456, 1–11, 2012.
6. Wigneron, J.-P., T. Schmugge, A. Chanzy, J.-C. Calvet, and Y. Kerr, "Use of passive microwave remote sensing to monitor soil moisture," *Agronomie*, Vol. 18, 27–43, 1998.
7. Barrett, B. W., E. Dwyer, and P. Whelan, "Soil moisture retrieval from active space borne microwave observations: An evaluation of current techniques," *Remote Sensing*, 210–242, 2019.
8. Das, H. P., "Satellite-based agro-advisory service," *Satellite Remote Sensing and GIS Applications in Agricultural Meteorology*, 347–359, 2013.
9. Mattikalli, N. M. and E. T. Engman, "Microwave remote sensing and GIS for monitoring surface soil moisture and estimation of soil properties," *Remote Sensing and Geographic Information Systems for Design and Operation of Water Resources on Systems*, 229–236, 1997.
10. Fabbro, V., C. Bourlier, and P. F. Combes, "Forward propagation modeling above Gaussian rough surfaces by the parabolic wave equation: Introduction of the shadowing effect," *Progress In Electromagnetics Research*, Vol. 58, 243–269, 2006.
11. Skidmore, A., *Environment Modelling with GIS and Remote Sensing*, Taylor and Francis, New York, ISBN: 0-415- 24170-7, 2003.
12. Ulaby, F. T., P. P. Batlivala, and M. C. Dobson, "Microwave backscatter dependence on surface roughness in soil moisture and soil texture, Part I — Bare Soil," *IEEE Transactions on Geoscience and Remote Sensing*, Vol. 16, 286–295, 1978.
13. Dubois, P. C., J. Van Zyl, and T. Engman, "Measuring soil moisture with imaging radars," *IEEE Transactions on Geoscience and Remote Sensing*, Vol. 33, 915–926, 1995.
14. Shi, J., J. Wang, A. Y. Hsu, E. O. O'neill, and E. T. Engman, "Estimation of bare surface soil moisture and surface roughness parameter using L-band SAR image data," *IEEE Transactions on Geoscience and Remote Sensing*, Vol. 35, 1254–1266, 1997.
15. Gruhier, C., P. de Rosnay, S. Hasenauer, T. Holmes, R. de Jeu, Y. Kerr, E. Mougin, E. Njoku, F. Timouk, W. Wagner, and M. Zribi, "Soil moisture active and passive microwave products: Intercomparison and evaluation over a sahelian site," *Hydrol. Earth Syst. Sci.*, Vol. 14, 141–156, 2010.
16. Ulaby, F. T., R. K. Moore, and A. K. Fung, *Microwave Remote Sensing: Active and Passive*, Artech House Inc., Dedham, MA, USA, 1986.
17. Ulaby, F. T., K. Sarabandi, K. Mcdonald, and M. C. Dobson, "Michigan microwave canopy scattering model," *Int. Journal of Remote Sensing*, Vol. 11, 1223–1253, 1990.
18. Attema, E. P. W. and F. T. Ulaby, "Vegetation modeled as a water cloud," *Radio Sci.*, Vol. 13, 357–364, 1978.
19. Roger, D., D. Roo, Y. Du, F. T. Ulaby, and M. C. Dobson, "A semi-empirical backscattering model at L-band and C-band for A soybean canopy with soil moisture inversion," *IEEE Transactions on Geoscience and Remote Sensing*, Vol. 39, 864–872, 2001.
20. Aubert, M., N. Baghdadi, M. Zribi, A. Douaoui, C. Loumagne, F. Baup, M. El Hajj, and S. Garrigues, " Analysis of TerraSAR-X data sensitivity to bare soil moisture, roughness, composition and soil crust," *Remote Sensing Environment*, Vol. 115, 1801–1810, 2011.
21. El Hajj, M., N. Baghdadi, M. Zribi, and H. Bazzi, "Synergic use of Sentinel-1 and Sentinel-2 images for operational soil moisture mapping at high spatial resolution over agricultural areas," *Remote Sensing*, Vol. 9, 1–28, 2017.

22. Gao, Q., M. Zribi, M. Escorihuela, and N. Baghdadi, "Synergetic use of Sentinel-1 and Sentinel-2 data for soil moisture mapping at 100 m resolution," *Sensors*, Vol. 17, No. 9, 1–21, 2017.
23. Paloscia, S., S. Pettinato, E. Santi, C. Notarnicola, L. Pasolli, and A. Reppucci, "Soil moisture mapping using Sentinel-1 images: Algorithm and preliminary validation," *Remote Sensing Environment*, Vol. 134, 234–248, 2013.
24. Zribi, M., A. Gorrab, N. Baghdadi, Z. Lili-Chabaane, and B. Mougenot, "Influence of radar frequency on the relationship between bare surface soil moisture vertical profile and radar backscatter," *Geoscience and Remote Sensing Letter*, Vol. 11, 848–852, IEEE, 2013.
25. Prakash, R., D. Singh, and N. P. Pathak, "The effect of soil texture in soil moisture retrieval for specular scattering at C-band," *Progress In Electromagnetics Research*, Vol. 108, 177–204, 2010.
26. Ballester-Berman, J. D., F. Vicente-Guijalba, and J. M. Lopez-Sanchez, "Polarimetric SAR model for soil moisture estimation over vineyards at C-band," *Progress In Electromagnetics Research*, Vol. 142, 639–665, 2013.
27. Panciera, R., M. A. Tanase, K. Lowell, and J. P. Walker, "Evaluation of IEM, Dubois, and Oh radar backscatter models using airborne L-band SAR," *IEEE Transactions on Geoscience and Remote Sensing*, Vol. 52, 4966–4979, 2014.
28. Singh, D. and A. Kathpalia, "An efficient modeling with GA approach to retrieve soil texture, moisture and roughness from ERS-2 SAR data," *Progress In Electromagnetics Research*, Vol. 77, 121–136, 2007.
29. Kasischke, E. S., J. M. Melack, and M. C. Dobson, "The use of imaging radars for ecological applications — A review," *Remote Sensing of Environment*, Vol. 59, 141–156, 1997.
30. Li, Z., W. Z. Liu, X. C. Zhang, and F. L. Zheng, "Impacts of land use change and climate variability on hydrology in an agricultural catchment on the Loess Plateau of China," *Journal of Hydrology*, Vol. 377, 35–42, 2009.
31. Feng, X. M., B. J. Fu, S. Piao, S. Wang, P. Ciais, Z. Z. Zeng, Y. H. Lu, Y. Zeng, Y. Li, X. H. Jiang, and B. F. Wu, "Revegetation in China's Loess Plateau is approaching sustainable water resource limits," *Nat. Clim. Chang.*, Vol. 6, 1019–1022, 2016.
32. Gao, X. D., H. C. Li, X. N. Zhao, W. Ma, and P. T. Wu, "Identifying a suitable revegetation technique for soil restoration on water-limited and degraded land: Considering both deep soil moisture deficit and soil organic carbon sequestration," *Geoderma*, Vol. 319, 61–69, 2018.
33. Dobos, E., "Albedo," *Encyclopedia of Soil Science*, 1–3, 2003.
34. Zribi, M., T. Baghdadi, N. Holah, and O. Fafin, "New methodology for soil surface moisture estimation and its application to ENVISAT-ASAR multi-incidence data inversion," *Remote Sensing of Environment*, Vol. 96, 485–496, 2005.
35. Malik, M. S. and J. P. Shukla, "Estimation of soil moisture by remote sensing and field methods: A review," *International Journal of Remote Sensing & Geoscience*, Vol. 3, No. 4, 21–27, 2014.
36. Attema, E. P. W. and F. T. Ulaby, "Vegetation modeled as a water cloud," *Radio Science*, Vol. 13, 357–364, 1978.
37. Lakhankar, T., N. Krakauer, and R. Khanbilvardi, "Applications of microwave remote sensing of soil moisture for agricultural applications," *International Journal of Terra space Science and Engineering*, Vol. 2, No. 1, 81–91, 2009.
38. Mekonnen, D. F., "Satellite remote sensing for soil moisture estimation, Gumara catchment, Ethiopia," Master Thesis, International Institute for Geo-Information Science and Earth Observation, Enschede, Netherlands, 2009.
39. Copernicus Space Component Data Access Portal: <https://scihub.copernicus.eu/dhus/#/home>.
40. U.S. Geological Survey 'EarthExplorer' website : <https://earthexplorer.usgs.gov/>.
41. Kirimi, F. D. N. Kuria, F. Thonfeld, E. Amler, K. Mubea, S. Misana, and G. Menz, "Influence of vegetation cover on the oh soil moisture retrieval model: A case study of the Malinda Wetland Tanzania," *Advances in Remote Sensing*, Vol. 5, 28–42, 2016.

42. El Hagg, M., N. Baghdadi, M. Zribi, G. Belaud, B. Cheviron, D. Courault, and F. Charron, "Soil moisture retrieval over irrigated grassland using X-band SAR data," *Remote Sensing Environment*, Vol. 176, 202–218, 2016.
43. Şekertekin, A., A. M. Marangoz, and S. Abdikan, "Soil moisture mapping using Sentinel-1A synthetic aperture radar data," *International Journal of Environment and Geoinformatics*, Vol. 5, No. 2, 178–188, 2016.